

Newton and Secant Methods for Iterative Remnant Control of Preisach Hysteresis Operators

J.R. Keulen, *Graduate Student Member, IEEE*, B.Jayawardhana, *Senior Member, IEEE*

Abstract—We study the properties of remnant function, which is a function of output remnant versus amplitude of the input signal, of Preisach hysteresis operators. The remnant behavior (or the leftover memory when the input reaches zero) enables an energy-optimal application of piezoactuator systems where the applied electrical field can be removed when the desired strain/displacement has been attained. We show that when the underlying weight of Preisach operators is positive, the resulting remnant curve is monotonically increasing and accordingly a Newton and secant update laws for the iterative remnant control are proposed that allows faster convergence to the desired remnant value than the existing iterative remnant control algorithm in literature as validated by numerical simulation.

Index Terms—Hysteresis, Preisach hysteresis operator, Remnant control, Mechatronics, Newton's method

I. INTRODUCTION

HYSTERESIS is a phenomenon where the response of a system depends not only on its current input but also on the past and present memory of its state. Hysteresis behaviors are commonly encountered in materials with memory, for example, in ferromagnetic, shape memory alloy, and piezoelectric systems. It is important to study hysteretic behavior to control such systems.

There are multiple mathematical models discussed in the literature to describe hysteretic behavior. Depending on whether the hysteresis behavior is affected by the rate of the input, one can have rate-independent hysteresis models and the rate-dependent ones. Rate-dependent hysteretic behavior can, for example, be modeled by non-smooth integrodifferential equations, such as the Duhem models [1], although they have also been used to represent rate-independent hysteretic behavior. Other models are based on infinite-dimensional operators, which include the well-studied Preisach operators. The Preisach operators are constructed from an infinite number of hysterons, which are typically given by relay operators [2]. There are a number of variations of the Preisach operators, such as the Krasnosel'skii–Pokrovskii (KP) operators [3], the

Prandtl-Ishlinskii [4] and many others. We refer the interested readers to the exposition on hysteresis models in [5]–[7].

Various control methods for hysteretic systems are discussed in the literature. The general objective is to employ hysteresis models, such as the standard Preisach operators, to accurately represent the system's behavior. Subsequently, the inverse of this hysteresis model is integrated into feedforward control methodologies to compensate for the unwanted hysteretic behavior [8] or to use an internal property of hysteresis, such as, energy dissipation [9] or sector-bound conditions to conclude systems' stability [10], [11]. In [4], the authors utilized the rate-dependent Prandtl-Ishlinskii hysteresis model to design a nonlinear controller containing an inverse multiplicative structure of the hysteresis model. By studying the time-derivative of input and output of hysteresis operators as in [10], [12], [13], feedback stability of hysteretic systems can be concluded via absolute stability analysis. Feedback control analysis and design that relies on the inherent energy dissipativity property of general hysteresis operators (given by either the Preisach or Duhem models) is presented in [14], [15]. An inversion-free feedforward hysteresis control approach is found in [16]. In all these works, the output regulation of a constant reference point requires a constant control input to the (hysteretic) actuator. Consequently, a constant consumption of power is needed and it can lead to engineering design difficulty when a large number of such actuators are used for particular high-tech applications, such as, the high-density deformable mirror proposed in [17], [18].

In contrast to having an active control for achieving output regulation of hysteretic systems as above, we study in this paper the problem of output remnant control where the control input can be set to zero when the desired output has been reached; thanks to the hysteresis' remnant property. Generally speaking, the output remnant is the leftover memory of the hysteresis when the input is set to zero. Depending on the input history or memory of the hysteresis, the output remnant can take any value from an admissible remnant interval. In this regard, the output remnant control corresponds to designing an admissible input signal that can bring the output remnant from an initial remnant value to a desired remnant state. As described before, the control of this remnant value is relevant for applications that require minimal use of input control due to various factors, such as, complex power electronics design for controlling high-density hysteretic actuators, power constraint, or the consequent energy loss/heat dissipation associated with

This research project is supported by a TKI (Topconsortia voor Kennis en Innovatie) grant within the Top Sector High-Tech Systems and Materials (HTSM).

J.R. Keulen and B. Jayawardhana are with the Engineering and Technology Institute Groningen, Faculty of Science and Engineering, University of Groningen, 9747AG Groningen, The Netherlands (e-mails: j.r.keulen@rug.nl, b.jayawardhana@rug.nl)

the use of a constant non-zero input to sustain the desired output. An example of such application in the high-precision opto-mechatronics systems that exploit such output remnant behaviors is the development of hysteretic deformable mirror for space application [17]. The deformable mirror uses a Nb-doped piezo material (PZT), which allows a wide range of remnant deformation [19]. In order to address the remnant control problem in these applications, a recursive remnant control algorithm has been proposed in [20] that is based on a standard iterative learning control law where the input amplitude is updated proportional to the remnant error. The learning rate / gain affects the convergence rate of the remnant control and it cannot be set arbitrary fast without inducing instability.

In this paper, we study the remnant property of Preisach hysteresis operators that will allow us to design an output remnant control law with better transient performance. Firstly, we investigate the property of remnant curve of such operators as a function of input amplitude for a given initial memory state. Secondly, based on the continuity and monotonicity property of the remnant curve, we propose a new iterative remnant control algorithm based on Newton and Secant methods.

The rest of this paper is structured as follows. In Section II we introduce the Preisach operators and the remnant control problem formulation. In Section III, we study some mathematical properties of the remnant curve of the Preisach operators. Subsequently, a new iterative remnant control algorithm is introduced in Section IV and its numerical validation is presented in Section V.

II. PREISACH HYSTERESIS OPERATORS AND REMNANT CONTROL PROBLEM

We denote $C(U, Y)$, $AC(U, Y)$, and $C_{pw}(U, Y)$ as the sets of continuous, absolutely continuous, and piece-wise continuous functions $f : U \rightarrow Y$, respectively. The space of p -integrable measurable functions $f : U \rightarrow Y$ is denoted by $\mathcal{L}^p(U, Y)$. The Sobolev space $W^{k,p}(U, Y)$ is a subset of measurable functions $f \in L^p(U, Y)$ where its weak-derivatives up to order k belong also to $L^p(U, Y)$.

A. Preisach hysteresis operator

Let us present a formal definition of standard Preisach operators, as presented in [2]. For this purpose, we firstly define the Preisach plane P by $P := \{(\alpha, \beta) \in \mathbb{R}^2 | \alpha \geq \beta\}$. In this plane, an interface line can be defined that separates the relays of Preisach operator (which will be defined shortly) which have positive values and the ones with negative values. Specifically, an interface line L is defined by monotonically increasing sequences $\alpha_i \geq 0$ and $\beta_i \geq 0$, $i \in \mathbb{N}$ with $\alpha_1 = \beta_1 = 0$, and is given by

$$L := \left\{ \begin{array}{l} \bigcup_{i \in \mathbb{N}} ([\alpha_i, \alpha_{i+1}] \times \{-\beta_i\}) \cup (\{\alpha_{i+1}\} \times [-\beta_{i+1}, -\beta_i]) \\ \bigcup_{i \in \mathbb{N}} (\{\alpha_i\} \times [-\beta_{i+1}, -\beta_i]) \cup ([\alpha_i, \alpha_{i+1}] \times \{-\beta_{i+1}\}) \end{array} \right\}. \quad (1)$$

Roughly speaking, the interface is a staircase line that starts from $(0, 0)$ with horizontal or vertical sub-lines, and is defined only in the second quadrant of the Preisach plane P , i.e. in $\mathbb{R}_- \times \mathbb{R}_+ =: P_2$. Let us denote by \mathcal{I} the set of all interface

lines $L \in P_2$. For a given initial interface L_0 , the Preisach operator $\mathcal{P} : AC(\mathbb{R}_+, \mathbb{R}) \times \mathcal{I} \rightarrow AC(\mathbb{R}_+, \mathbb{R})$ can be formally defined by

$$(\mathcal{P}(u, L_0))(t) := \iint_{(\alpha, \beta) \in P} w(\alpha, \beta) (\mathcal{R}_{\alpha, \beta}(u, L_0))(t) d\alpha d\beta \quad (2)$$

where $w : \mathbb{R} \rightarrow \mathbb{R}_+$ is the weight function, and $\mathcal{R}_{\alpha, \beta}(u, L_0)$ is the relay operator defined by

$$(\mathcal{R}_{\alpha, \beta}(u))(t) := \begin{cases} 1 & \text{if } u(t) > \alpha, \\ -1 & \text{if } u(t) < \beta, \\ (\mathcal{R}_{\alpha, \beta}(u))(t_-) & \text{if } \beta \leq u(t) \leq \alpha, t > 0, \\ r_{\alpha, \beta}(L_0) & \text{if } \beta \leq u(t) \leq \alpha, t = 0, \end{cases}$$

where we omit the argument of L_0 in the definition for conciseness and $r_{\alpha, \beta}(L_0)$ is the initial state of the relay $\mathcal{R}_{\alpha, \beta}$ which is equal to -1 if (α, β) is located above L_0 and 1 otherwise.

For $h \geq 0$ and $\mathbb{R}_h := [-h, \infty)$, a function $f : \mathbb{R}_h \rightarrow \mathbb{R}_h$ is a *time transformation* if f is continuous and non-decreasing with $f(-h) = -h$ and $\lim_{t \rightarrow \infty} f(t) = \infty$; in other words f is a time transformation if it is continuous, non-decreasing and subjective. Following the work of [21], the Preisach operator \mathcal{P} is *rate independent*, i.e. for every time transformation f it holds that

$$(\mathcal{P}(u \circ f))(t) = (\mathcal{P}(u))(f(t)), \quad \forall u \in C(\mathbb{R}_h), \quad \forall t \in \mathbb{R}_h. \quad (3)$$

B. Remnant control problem for Preisach operators

In general, for any given desired remnant position y_d , the remnant control problem pertains to the design of input signal u , where $u(t) = 0$ for all $t > T$ for some $T > 0$ and $u(t) \neq 0$ on $(0, T)$, such that the corresponding output of the hysteresis operator will be equal to y_d after the input is set to zero (i.e. after time T). For the Preisach operator with a given initial interface $L_0 \in \mathcal{I}$, the application of such input signal u should lead to $\mathcal{P}(u, L_0)(t) = y_d$ for all $t \geq T$. Intrinsically, the input signal u alters the interface function such that some relays in the Preisach domain P have switched from the initial state $r_{\alpha, \beta}$ so that the remnant value is equal to y_d .

Let $L_T \in \mathcal{I}$ be the final interface that describes the state of the relays in the Preisach operator at $t = T$ and correspondingly, we define $P_T \subset P$ be the domain of relays $\mathcal{R}_{\alpha, \beta}$ that have switched their value from their initial condition $r_{\alpha, \beta}$ that depends on L_0 . Using P_T , the challenge of remnant control is on the design of a feedforward control input u such that its values are zero at a given terminal time T and the remnant output that is due to the switched relays in P_T is equal to the required incremental output needed to bring the initial output y_0 to the desired one y_d .

In [20] an iterative algorithm is proposed based on an input of the form

$$u(t) := \sum_{k=0}^{\infty} A_k v_k(t), \quad (4)$$

where v_k is a triangular pulse signal with a unit amplitude whose pulse starts at $t = kT$ and vanishes at $t = (k+1)T$ with T be the periodic remnant update time and A_k be the amplitude for the k -th pulse. The input u can be seen as a

sequence of triangular pulses whose amplitudes are modulated by A_k . By the application of such input signal, the remnant output after the application of the k -th triangular wave $A_k v_k(t)$ is given by

$$y_k := \left(\mathcal{P}(u, L_0) \right) \left((k+1)T \right) = \left(\mathcal{P}(A_k v_k, L_k) \right) (T). \quad (5)$$

As studied in [20], the iterative remnant control design problem corresponds to the design of an update rule for the amplitude A_{k+1} based on the current amplitude A_k and remnant value y_k such that y_k converges to y_d as $k \rightarrow \infty$. Particularly, the update rule that is studied in [20] is given by

$$A_{k+1} = A_k - \lambda e_k, \quad (6)$$

where $e_k = y_k - y_d$ is the remnant error and λ is the adaptation gain. A bound on the adaptation gain λ is further studied in [20] that guarantees the convergence of A_k in (6) to the desired amplitude for attaining the desired remnant position. This convergence property relies on a monotonicity property of the remnant position as a function of the input amplitude A . This method relies on a constant gain value, which can limit the convergence speed to the desired remnant position. With the introduction of the remnant curve, where we investigate the mapping between the amplitude A and the remnant value, we can introduce a new remnant control algorithm that exploits an adaptive gain in the form of the Newton method.

III. REMNANT CURVE AND ITS PROPERTIES

Let us firstly define the remnant curve $\rho_{L_0} : \mathbb{R} \rightarrow \mathbb{R}$, that maps the input amplitude (defined shortly below) to the remnant position. Note that the remnant curve, in this case, is dependent on the initial interface line L_0 . For a different initial interface line, the remnant curve will be different. Let $v(A, t) : \mathbb{R} \times \mathbb{R} \rightarrow \mathbb{R}$ be a piecewise-continuous input parametrized by the amplitude A such that there exist a $T_2 > T_1 > 0$ so that the following conditions hold:

- R1. $v(A, 0) = 0$ and $v(A, t) = 0$ for all $t \geq T_2$;
- R2. $v(A, t)$ is monotone on each time interval $t \in (0, T_1)$ and $t \in (T_1, T_2)$;
- R3. $\frac{d}{dt} v(A, T_1) \frac{d}{dt} v(A, T_2) < 0$ for all $T_1 \in (0, T_1)$ and $T_2 \in (T_1, T_2)$;
- R4. $\text{sign}\left(\frac{d}{dt} v(A, T_1)\right) = \text{sign}(A)$.

Using the above input signal $v_\rho(A, t)$, the remnant curve ρ_{L_0} can then be defined by

$$\rho_{L_0}(A) = \lim_{t \rightarrow \infty} (\mathcal{P}(v(A, \cdot), L_0))(t). \quad (7)$$

Note that we use the asymptotic value in the above definition so that it is independent of a particular value of T_2 , which may not be unique. One can also replace the asymptotic value in the above definition if one fixes the value of T_2 when we design the *feedforward remnant input* as will be used later in Section IV. In this case, we can modify (7) into

$$\rho_{L_0}(A) = (\mathcal{P}(v(A, \cdot), L_0))(T), \quad (8)$$

where T is the time at which $v(A, T) = 0$. The initial remnant value is trivially given by $\rho_{L_0}(0)$. Due to the rate-independent property of the Preisach operator, one can immediately check that ρ_{L_0} is invariant to the particular form of v_ρ as shown in the following proposition.

Proposition III.1. *Consider a Preisach operator \mathcal{P} as in (2) with a given weight function w and initial interface L_0 . For any initial interface L_0 , the corresponding remnant curve ρ_L is invariant to the particular form of $v(A, t)$ satisfying R1 – R4.*

PROOF. We will prove this proposition by showing that for any pair of $v_1(A, t)$ and $v_2(A, t)$, we have

$$\lim_{t \rightarrow \infty} (\mathcal{P}(v_1(A, \cdot), L_0))(t) = \lim_{t \rightarrow \infty} (\mathcal{P}(v_2(A, \cdot), L_0))(t)$$

for all $A \in \mathbb{R}$.

As shown before, the Preisach operator has rate-independent property, namely, for all time transformation f , it holds that

$$\left(\mathcal{P}(v_1(A, \cdot) \circ f) \right) (t) = \left(\mathcal{P}(v_1(A, \cdot)) \right) (f(t)). \quad (9)$$

By the monotonicity of v_1 on the time intervals $(0, T_{1,v_1})$ and (T_{1,v_1}, T_{2,v_1}) and the monotonicity of v_2 on the time intervals $(0, T_{1,v_2})$ and (T_{1,v_2}, T_{2,v_2}) , we can define a time transformation f for every A such that $v_1(A, f(t)) = v_2(A, t)$ for all $t \geq 0$. In this case, (9) becomes

$$\left(\mathcal{P}(v_2(A, \cdot)) \right) (t) = \left(\mathcal{P}(v_1(A, \cdot)) \right) (f(t)).$$

By taking $t \rightarrow \infty$, we establish our claim. \square

Proposition III.1 leads to the conclusion that the amplitude of the input signal serves as the variable parameter in the remnant control problem. The subsequent proposition follows from the wiping-out property of the Preisach hysteresis model and discusses how the interface evolves after the application of such input signal.

Proposition III.2. *Consider a Preisach operator \mathcal{P} as in (2) with a given weight function w and initial interface L_0 whose staircase line is defined by the sequences $\{\alpha_{i,0}\}_{i \in \mathbb{N}}$ and $\{\beta_{i,0}\}_{i \in \mathbb{N}}$ as in (1). Then the new interface line L_1 (with the sequences $\{\alpha_{i,1}\}_{i \in \mathbb{N}}$ and $\{\beta_{i,1}\}_{i \in \mathbb{N}}$) after the application of input signal $u(t) = v(A, t)$ to \mathcal{P} satisfies $\alpha_{1,1} = \beta_{1,1} = 0$ and*

- if $A > \alpha_{2,0}$ then

$$\alpha_{2,1} = A, \quad \alpha_{i,1} = \alpha_{i+k_1-3,0} \quad \forall i \geq 3$$

$$\beta_{i,1} = \beta_{i+k_2,0} \quad \forall i \geq 2$$

- otherwise (i.e. if $A < -\beta_{2,0}$)

$$\alpha_{i,1} = \alpha_{i+k_3,0} \quad \forall i \geq 2$$

$$\beta_{2,1} = -A, \quad \beta_{i,1} = \beta_{i+k_4-3,0} \quad \forall i \geq 3,$$

where k_2, k_3 are the indices of $\alpha_{i,0}$ and $\beta_{i,0}$ such that $(A, -\beta_{i+k_2,0}) \in L_0$ and $(\alpha_{i+k_3,0}, -A) \in L_0$, respectively, and k_1, k_4 are the smallest indices of $\alpha_{i,0}$ and $\beta_{i,0}$ such that $\alpha_{k_1,0} > |A|$ and $\beta_{k_4,0} > |A|$.

PROOF. We start the proof by analyzing the changes to the interface line when $A > \alpha_{2,0}$. The other case can be proven in a similar fashion.

Firstly, when the input signal has reached its maximum value of A , all relays $\mathcal{R}_{\alpha,\beta}$ with $\alpha < A$ will switch to 1. This implies that the horizontal and vertical lines of the interface that are associated to the sequence $\alpha_{i,0} < A$, $i \neq 0$ will be wiped out in the new interface and it creates a new horizontal line with $\alpha_{2,1} = A$. The rest of the new sequence $\alpha_{i,1}$ with $i > 1$ will follow the sequence from the original one that is not wiped out, i.e., those associated to $\alpha_{i+k_1-1,0}$. Subsequently,

when the input signal returns back to 0, all relays $\mathcal{R}_{\alpha,\beta}$ with $\beta > 0$ will be at -1 state and the vertical lines of the interface will be redrawn to the vertical line of L_0 that contains the element $(A, -\beta_{i,0})$ for some $i > 1$ and all $\beta_{j,0}$ s.t. $\beta_{j,0} < \beta_{i,0}$ will be wiped out. \square

In Proposition III.2, the removal of elements in the sequence of α and β from the original one when the input $v(A, t)$ is applied to the Preisach operator is known in the literature as the *wiping-out* property. The characterization of this wiping-out property will be useful to get the relationship between the remnant value and the weights of the Preisach operator associated to the wiped-out domain.

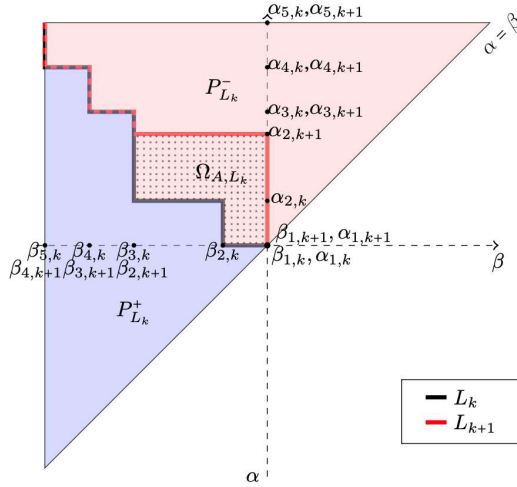


Fig. 1: Preisach domain with a particular staircase interface L_0 , consisting of the sequence $\{\alpha_{1,k}, \alpha_{2,k}, \alpha_{3,k}, \alpha_{4,k}, \alpha_{5,k}\}$ and $\{\beta_{1,k}, \beta_{2,k}, \beta_{3,k}, \beta_{4,k}, \beta_{5,k}\}$, after application of input signal with $A_k = \alpha_{2,k+1}$ some horizontal and vertical lines of L_k are wiped out, resulting in the new interface L_{k+1} consisting of the sequence $\{\alpha_{1,k+1}, \alpha_{2,k+1}, \alpha_{3,k+1}, \alpha_{4,k+1}, \alpha_{5,k+1}\}$ and $\{\beta_{1,k+1}, \beta_{2,k+1}, \beta_{3,k+1}, \beta_{4,k+1}\}$.

Figure 1 shows an example of vertices being wiped out after an application of an input signal $v(A_k, t - kT)$, where amplitude $A_k = \alpha_{2,k+1}$. We can define a new region between L_k and L_{k+1} , where the relay switched from -1 to $+1$. For the rest of this paper, we will denote this region by Ω_{A,L_k} .

Proposition III.3. Consider a Preisach operator \mathcal{P} as in (2) with a given weight function w , initial interface L_k and the input signal $v(A, t)$ satisfying R1-R4 with $T_2 = T$. Then the corresponding remnant curve ρ_{L_k} is given by

$$\rho_{L_k}(A) = \iint_{(\alpha,\beta) \in \Omega_{A,L_k}} w(\alpha, \beta) d\alpha d\beta + \rho_0, \quad (10)$$

where region Ω_{A,L_k} is defined as the domain in P that is enclosed by L_k and $L_{k+1}(A)$ as given in Proposition III.2 and $\rho_0 \in \mathbb{R}$ is the initial remnant value due to L_k .

PROOF. As shown in Proposition III.1 the remnant curve is invariant to the particular form of $v(A, t)$. Applying such input signal to \mathcal{P} and using (2), we can compute (8) as follows

$$\rho_{L_k}(A) = \iint_{\beta \alpha} w(\alpha, \beta) \mathcal{R}_{\alpha,\beta}(v(A, \cdot))(T) d\alpha d\beta \quad (11)$$

where we have used $\mathcal{R}_{\alpha,\beta}(v(A, \cdot))(0) = r_{\alpha,\beta}(L_k)$ describing the initial state of the relay $\mathcal{R}_{\alpha,\beta}$ which is equal to -1 if (α, β) is located above L_k and 1 otherwise. Let $P_{L_k}^-$ and $P_{L_k}^+$ denote the subdomains of the Preisach domain P that are above or below the interface L_k . Let L_{k+1} denote the new interface of the Preisach plane after the application of input $v(A, t)$. Then the first term on the RHS of (11) can be expressed as

$$\begin{aligned} \iint_{\beta \alpha} w(\alpha, \beta) \mathcal{R}_{\alpha,\beta}(v(A, \cdot))(T) d\alpha d\beta &= - \iint_{P_{L_k}^-} w(\alpha, \beta) d\alpha d\beta \\ &+ \iint_{P_{L_k}^+} w(\alpha, \beta) d\alpha d\beta + \iint_{(\alpha,\beta) \in \Omega_{A,L_k}} w(\alpha, \beta) d\alpha d\beta, \end{aligned}$$

where the last term corresponds to the fact that the relays in Ω_{A,L_k} have changed their state from -1 to 1 due to the application of $v(A, t)$, and the sum of the first two terms is equal to the Preisach output when the interface L_k is used, i.e. it is equal to initial remnant value ρ_0 . \square

By utilizing the explicit definition of the remnant curve in (10), we can compute, under a specific assumption, the first derivative of $\rho_{L_k}(A)$ as a function of A . With this expression, we can study the sensitivity of the remnant curve with respect to the changes in the input signal amplitude.

Proposition III.4. Let L_k be an initial interface of \mathcal{P} whose weight function $w \in C(P, \mathbb{R}) \cap \mathcal{L}^1(P, \mathbb{R})$. Then $\rho_{L_k} \in W^{1,\infty}(P, \mathbb{R})$ (i.e. it is Lipschitz continuous).

PROOF. It follows from Proposition III.3 that $\rho_{L_k}(A)$ is given by (10). Following the analysis of hysteresis operator as in [9], let us define a weak-derivative of ρ_{L_k} using the upper-right Dini's derivative as follows

$$\begin{aligned} \frac{d}{dA} \rho_{L_k}(A) &:= \limsup_{h \rightarrow 0^+} \frac{\rho_{L_k}(A+h) - \rho_{L_k}(A)}{h} \\ &= \limsup_{h \rightarrow 0^+} \frac{\iint_{(\alpha,\beta) \in \Delta_h} w(\alpha, \beta) d\alpha d\beta}{h}, \end{aligned}$$

where the last equation is due to (10) and Δ_h is the domain defined by $\Omega_{A+h,L_k} - \Omega_{A,L_k}$. Firstly, when A is not at the boundary of the vertices of L_k , then it follows from the above equation and continuity of w that for $A > 0$,

$$\begin{aligned} \frac{d}{dA} \rho_{L_k}(A) &= \limsup_{h \rightarrow 0^+} \frac{\int_{-\beta_{i,k}}^0 \int_A^{A+h} w(\alpha, \beta) d\alpha d\beta}{h} \\ &= \int_{-\beta_{i,k}}^0 w(A, \beta) d\beta, \end{aligned}$$

with $i > 1$ be s.t. $(A, -\beta_{i,k}) \in L_k$, holds. Similarly, for $A < 0$,

$$\begin{aligned} \frac{d}{dA} \rho_{L_k}(A) &= \limsup_{h \rightarrow 0^+} \frac{\int_0^{A+h} \int_0^{\alpha_{i,k}} w(\alpha, \beta) d\alpha d\beta}{h} \\ &= \int_0^{\alpha_{i,k}} w(\alpha, A) d\alpha \end{aligned}$$

with $i > 1$ be s.t. $(\alpha_{i,k}, -A) \in L_k$ holds. For this case, one can also check that taking the other limits of Dini's derivative (lower-right, upper-left and lower-left) also leads to the same quantity as above.

On the other hand, when A is equal to one of the interface vertices (i.e., $\alpha_{i,k}$ or $-\beta_{i,k}$ with $i \geq 2$), the computation of upper-right Dini's derivative leads to

- For $A > 0$: $\frac{d}{dA}\rho_{L_k}(A) = \int_{-\beta_{i+1,k}}^0 w(A, \beta) d\beta$;
- For $A < 0$: $\frac{d}{dA}\rho_{L_k}(A) = \int_0^{\alpha_{i+1,k}} w(\alpha, A) d\alpha$,

with the same i as before. The jump of the derivative at the interface vertices is due to the discontinuity of the staircase interface function L . Since w is also \mathcal{L}^1 , we can conclude that ρ_{L_k} is Lipschitz continuous. \square

Proposition III.5. *If w is positive definite then for any given interface L_k the remnant curve ρ_{L_k} is monotone increasing.*

The proof follows directly from (10) where a growing $|A|$ implies also that the region Ω_{A,L_k} enlarges. Hence ρ_{L_k} is monotonically increasing.

IV. NEWTON & SECANT METHODS

Let us introduce iterative remnant input signals given by

$$u(t) = v(-A_{\max}, t) + \sum_{k=1}^{\infty} v(A_k, t - (2k-1)T) + v(-A_{\max}, t - 2kT), \quad (12)$$

where $v(A, t)$ is the input signal modulated by A and satisfies R1-R4 with $T_2 = T$, and the constant $A_{\max} > 0$ is a maximum remnant input amplitude. The first term and last term in (12) are reset sub-signals such that the interface at each iteration step k will be reset to $L_k = (\{0\} \times [-A_{\max}, 0]) \cup ([0, A_{\max}] \times \{-A_{\max}\}) \cup \dots$. Using this iterative remnant input signal, our main design problem is to define an update law for A_k such that A_k converges to the desired amplitude where the remnant value is equal to the desired one. Due to the particular reset sub-signals in (12), it is implicitly assumed that the desired remnant output y_d is larger than the remnant output after the initial reset signal but is still within the admissible range so that there exists $0 < A_d < A_{\max}$ such that $\rho_{L_1}(A_d) = y_d$. However, if y_d is smaller than the remnant output after the initial reset signal, we can reverse the sign of reset sub-signals into $v(A_{\max}, t)$ and $v(A_{\max}, t - 2kT)$ correspondingly, so that the target amplitude will satisfy $A_d < 0$. In both cases, we need to design an iterative remnant control such that $A_k \rightarrow A_d$. In the following analysis, we will consider the first case where we use (12) with $0 < A_d < A_{\max}$. For every iteration step k , define the remnant error e_k (as in (6)) by $e_k = \rho_{L_k}(A_k) - y_d$.

Theorem IV.1. *Consider a Preisach operator \mathcal{P} as in (2) with a positive-definite $w \in C^1(P, \mathbb{R}_+)$ and an initial interface L_0 . Consider an iterative remnant input signal u as in (12) with $A_{\max} > 0$, and let $y_d > \rho_{L_1}(0)$ be the desired remnant value with L_1 be the interface after the first reset sub-signal. Let A_k be updated by the following Newton's iterative remnant update law*

$$A_{k+1} = A_k - \frac{e_k}{\rho'_{L_k}(A_k)}, \quad (13)$$

where $\rho'_{L_k}(A_k)$ is the derivative of ρ_{L_k} as in Proposition III.4. Then for an initial amplitude A_1 sufficiently close to A_d , e_k converges quadratically to zero as $k \rightarrow \infty$ i.e. for some $\delta > 0$, $|A_{k+1} - A_d| \leq \delta |A_k - A_d|^2$. \square

PROOF. Due to the introduction of reset sub-signals in (12), the remnant curve ρ_{L_k} will be identical for every iterative step k within the interval $\mathcal{I} := [0, A_{\max})$ according to Proposition III.2 and we will simply denote it by ρ_L . Following the proof of Proposition III.4, the remnant curve ρ_L is C^1 in \mathcal{I} since its derivative is continuous and it is monotonically increasing following Proposition III.5. Particularly, $\frac{d}{dA}\rho_L(A) = \int_{-A_{\max}}^0 w(A, \beta) d\beta > 0$ and $\frac{d^2}{dA^2}\rho_L(A) = \int_{-A_{\max}}^0 \frac{d}{dA}w(A, \beta) d\beta$. Moreover, since $w \in C^1$, we also have that $\rho_L \in C^2$.

Let us denote $E_k = A_d - A_k$. By Taylor series, we have

$$0 = \rho_L(A_k) - y_d + \frac{d}{dA}\rho_L(A_k)(E_k) + \frac{d^2}{dA^2}\rho_L(\xi)(E_k)^2,$$

where $\xi \in [A_k, A_d]$. It follows from this equation that

$$\frac{\rho_L(A_k) - y_d}{\rho'_{L_k}(A_k)} + A_d - A_k = -\frac{\frac{d^2}{dA^2}\rho_L(\xi)}{\frac{d}{dA}\rho_L(A_k)}(A_d - A_k)^2.$$

Now subtracting both sides in (13) by A_d and substituting the above relation to the RHS term of (13), we arrive at

$|A_{k+1} - A_d| = \frac{\frac{d^2}{dA^2}\rho_L(\xi)}{\frac{d}{dA}\rho_L(A_k)}|A_k - A_d|^2$. By taking an initial amplitude A_1 close to A_d such that $\delta|E_1| < 1$ where $\delta = \kappa/\lambda$ with $\kappa = \sup_{\xi \in \mathcal{I}_E} \left| \frac{d^2}{dA^2}\rho_L(\xi) \right|$, $\lambda = \sup_{\xi \in \mathcal{I}_E} \left| \frac{d}{dA}\rho(\xi) \right|$, with $\mathcal{I}_E := [A_d - |E_1|, A_d + |E_1|] \subset \mathcal{I}$, we can guarantee the quadratic convergence of the iterative remnant update law (13) so that the inequality (14) holds. \square

The update law as in (13) is akin to the Newton's method. As it may be difficult to obtain numerically the gradient of the remnant curve ρ_L at each iteration, one can use an approximation of $\frac{d}{dA}\rho_L$ as follows, $\frac{d}{dA}\rho_L(A_k) \approx \frac{\rho_L(A_k) - \rho_L(A_{k-1})}{A_k - A_{k-1}}$, which is also known in the literature as the secant method. In this case, the secant-method iterative remnant update law is given by

$$A_{k+1} = A_k - \frac{A_k - A_{k-1}}{\rho_L(A_k) - \rho_L(A_{k-1})} e_k. \quad (15)$$

For both methods, when the underlying weight w is approximately constant, i.e. $w(\alpha, \beta) \approx C$ with $C > 0$, it follows from the computation in the proof of Theorem IV.1 that $\frac{d}{dA}\rho_L(A) \approx CA_{\max}$ and $\frac{d^2}{dA^2}\rho_L(A) \approx 0$ since $\frac{d}{dA}w(A, \beta) \approx 0$. In this case, we can admit initial amplitude A_1 that is far from A_d . This particular case is the one considered in the simulation results below.

As discussed earlier, we can also consider the complementary reset sub-signals in (12) using its signed reverse form. Similar results as in Theorem IV.1 can be obtained using the same Newton's iterative remnant control law (13) and its secant-method one in (15).

V. NUMERICAL SIMULATION

In this section, we perform numerical simulations of the Newton-based iterative remnant control to track a desired remnant output. We compare the transient response of Secant-based method (15) to the iterative control algorithm of [20]. For the simulation setup, we consider the Preisach operator as in (2) with randomly generated initial interface L_0 and with a uniform weight function w . For numerical purpose,

we discretize the Preisach plane into $N = 500500$ regularly spaced relays in the 2D plane of $[-400, 400] \times [-400, 400]$ with uniform constant weight of $1/N$. For the Monte Carlo simulation, we use 100 samples for each method, where a normally distributed desired remnant output with mean value of 0.1 and standard deviation of 0.0878 is considered to evaluate the efficacy of the proposed methods in tracking different desired remnant output values. We set $A_{\max} = 400$ which follows the considered Preisach plane. The initial amplitudes for the secant method are given by $A_0 = 50$ and $A_1 = 100$, and the initial amplitude for the iterative requires is set at $A_0 = 50$. In addition, three different gains are used for the original iterative remnant control method, to evaluate the influence of λ on the convergence rate. The resulting Monte Carlo simulation is shown in Figure 2 which shows a histogram of required iterations to converge to the randomly generated desired remnant output and the transient response of sample 1. This Monte Carlo simulation result shows that the secant-based iterative remnant control method converges faster in all cases to the desired remnant output than the previously proposed iterative remnant control method in [20].

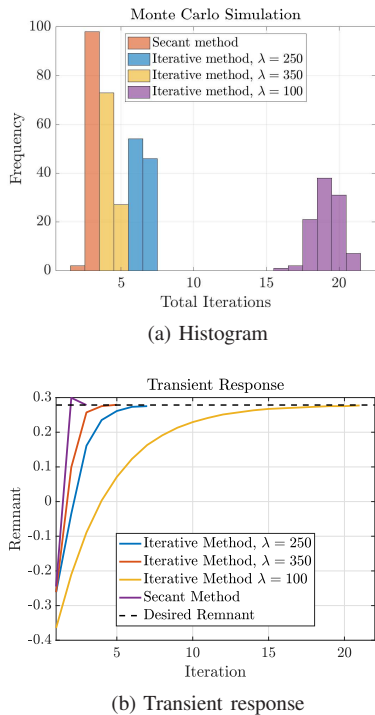


Fig. 2: Numerical simulation results, where the proposed secant-based iterative remnant control method is compared with the iterative remnant control method of [20] with different values for λ .

VI. CONCLUSIONS

In this paper, we studied the mathematical properties of the remnant curve and showed how these properties can be used to propose a new iterative remnant control law based on Newton and secant methods. Further works are underway on the generalization of the remnant control and its analysis to

the hysteresis with butterfly loops as studied in [19], where monotonicity of the remnant curve is no longer guaranteed.

REFERENCES

- [1] F. Ikhouane, "A survey of the hysteretic duhem model," *Archives of Computational Methods in Engineering*, vol. 25, no. 4, pp. 965–1002, 2018.
- [2] I. D. Mayergoyz, *Mathematical models of hysteresis and their applications*. Academic press, 2003.
- [3] M. A. Krasnosel'skii and A. V. Pokrovskii, *Systems with hysteresis*. Springer Science & Business Media, 2012.
- [4] M. Al Janaideh, M. Rakotondrabe, I. Al-Darabsah, and O. Aljanaideh, "Internal model-based feedback control design for inversion-free feedforward rate-dependent hysteresis compensation of piezoelectric cantilever actuator," *Control Engineering Practice*, vol. 72, pp. 29–41, 2018.
- [5] V. Hassani, T. Tjahjowidodo, and T. N. Do, "A survey on hysteresis modeling, identification and control," *Mechanical systems and signal processing*, vol. 49, no. 1-2, pp. 209–233, 2014.
- [6] A. Visintin, *Differential models of hysteresis*. Springer Science & Business Media, 2013, vol. 111.
- [7] M. Brokate and J. Sprekels, *Hysteresis and phase transitions*. Springer Science & Business Media, 1996, vol. 121.
- [8] R. V. Iyer, X. Tan, and P. S. Krishnaprasad, "Approximate inversion of the preisach hysteresis operator with application to control of smart actuators," *IEEE Transactions on automatic control*, vol. 50, no. 6, pp. 798–810, 2005.
- [9] B. Jayawardhana, R. Ouyang, and V. Andrieu, "Stability of systems with the duhem hysteresis operator: The dissipativity approach," *Automatica*, vol. 48, no. 10, pp. 2657–2662, 2012.
- [10] B. Jayawardhana, H. Logemann, and E. P. Ryan, "Pid control of second-order systems with hysteresis," *International Journal of Control*, vol. 81, no. 8, pp. 1331–1342, 2008.
- [11] —, "Input-to-state stability of differential inclusions with applications to hysteretic and quantized feedback systems," *SIAM Journal on Control and Optimization*, vol. 48, no. 2, pp. 1031–1054, 2009.
- [12] H. Logemann and E. P. Ryan, "Systems with hysteresis in the feedback loop: existence, regularity and asymptotic behaviour of solutions," *ESAIM: Control, Optimisation and Calculus of Variations*, vol. 9, pp. 169–196, 2003.
- [13] S. Tarbouriech, I. Queinnec, and C. Prieur, "Stability analysis and stabilization of systems with input backlash," *IEEE Transactions on Automatic Control*, vol. 59, no. 2, pp. 488–494, 2014.
- [14] R. B. Gorbet, K. A. Morris, and D. W. Wang, "Passivity-based stability and control of hysteresis in smart actuators," *IEEE Transactions on control systems technology*, vol. 9, no. 1, pp. 5–16, 2001.
- [15] R. Ouyang and B. Jayawardhana, "Absolute stability analysis of linear systems with duhem hysteresis operator," *Automatica*, vol. 50, no. 7, pp. 1860–1866, 2014.
- [16] M. Ruderman, "Inversion-free feedforward hysteresis control using preisach model," in *2023 European Control Conference (ECC)*. IEEE, 2023, pp. 1–6.
- [17] R. Huisman, M. P. Bruijn, S. Damerio, M. Eggen, S. N. Kazmi, A. E. Schmerbauch, H. Smit, M. A. Vasquez-Beltran, E. Van der Veer, M. Acuautila *et al.*, "High pixel number deformable mirror concept utilizing piezoelectric hysteresis for stable shape configurations," *Journal of Astronomical Telescopes, Instruments, and Systems*, vol. 7, no. 2, pp. 029002–029002, 2021.
- [18] A. Schmerbauch, M. Vasquez-Beltran, A. I. Vakis, R. Huisman, and B. Jayawardhana, "Influence functions for a hysteretic deformable mirror with a high-density 2d array of actuators," *Applied Optics*, vol. 59, no. 27, pp. 8077–8088, 2020.
- [19] B. Jayawardhana, M. V. Beltran, W. Van De Beek, C. de Jonge, M. Acuautila, S. Damerio, R. Peletier, B. Noheda, and R. Huisman, "Modeling and analysis of butterfly loops via preisach operators and its application in a piezoelectric material," in *2018 IEEE Conference on Decision and Control (CDC)*. IEEE, 2018, pp. 6894–6899.
- [20] M. Vasquez-Beltran, B. Jayawardhana, and R. Peletier, "Recursive algorithm for the control of output remnant of preisach hysteresis operator," *IEEE Control Systems Letters*, vol. 5, no. 3, pp. 1061–1066, 2020.
- [21] H. Logemann, E. P. Ryan, and I. Shvartsman, "A class of differential-delay systems with hysteresis: asymptotic behaviour of solutions," *Nonlinear Analysis: Theory, Methods & Applications*, vol. 69, no. 1, pp. 363–391, 2008.

